PHILOSOPHICAL TRANSACTIONS OF THE ROYAL SOCIETY A

Phil. Trans. R. Soc. A (2012) **370**, 1352–1375
doi:10.1098/rsta.2011.0276

Review

Titanium-containing bioactive phosphate glasses

By A. Kiani[1], N. J. Lakhkar[1], V. Salih[1], M. E. Smith[2], J. V. Hanna[2], R. J. Newport[3], D. M. Pickup[3] and J. C. Knowles[1,4,*]

[1]*Division of Biomaterials and Tissue Engineering, University College London Eastman Dental Institute, 256 Gray's Inn Road, London WC1X 8LD, UK*
[2]*Department of Physics, University of Warwick, Coventry CV4 7AL, UK*
[3]*School of Physical Sciences, University of Kent, Ingram Building, Canterbury CT2 7NH, UK*
[4]*Department of Nanobiomedical Science and WCU Research Center, Dankook University Graduate School, Cheonan 330-714, South Korea*

The use of biomaterials has revolutionized the biomedical field and has received substantial attention in the last two decades. Among the various types of biomaterials, phosphate glasses have generated great interest on account of their remarkable bioactivity and favourable physical properties for various biomedical applications relating to both hard and soft tissue regeneration. This review paper focuses mainly on the development of titanium-containing phosphate-based glasses and presents an overview of the structural and physical properties. The effect of titanium incorporation on the glassy network is to introduce favourable properties. The biocompatibility of these glasses is described along with recent developments in processing methodologies, and the potential of Ti-containing phosphate-based glasses as a bone substitute material is explored.

Keywords: biomaterials; glass; phosphate

1. Introduction

Biomaterials are artificial or natural materials that are used to replace lost or diseased tissue and to restore form and function. Thus, the field of biomaterials has become an imperative area, as these materials are helpful in improvement of the quality and the longevity of human life.

Phosphate-based glasses show unique features such as low melting (T_m) and glass transition (T_g) temperatures and high coefficients of thermal expansion that extend their applications in various technological fields [1–3]. Phosphate glasses have attracted huge interest recently as degradable biomaterials. These glasses have the unique property of being completely soluble in aqueous media, and, more importantly, this degradability can be controlled, with solubility times ranging

*Author for correspondence (j.knowles@ucl.ac.uk).

One contribution of 11 to a Theme Issue 'Structure and biological activity of glasses and ceramics'.

from a few hours to several months, to suit the end application via changes in the glass chemistry [4–8]. This ability to dissolve and to be able to control the rate is seen as a very desirable property, particularly for tissue engineering applications, in which the presence of a device is only required to support the cells/tissue in the short term. The main constituent of phosphate glasses is phosphorus pentoxide, which acts as the primary network former. However, pure vitreous P_2O_5 is very difficult to obtain in a glassy form. This is due to the fact that P_2O_5 is very hygroscopic and volatile; hence, a mixture of oxides including network modifiers and network intermediates are added to the phosphate glass system to stabilize the glass network [9,10].

Thus far, various metal oxides have been incorporated into the glass composition to control the degradability and associated properties, and, among all these, titanium dioxide (TiO_2) was shown to be highly favourable [4,7,11–35].

The first part of this review will present a brief description of the basic structure of phosphate-based glasses, followed by an overview of the role of titanium in the phosphate glass structure and how its inclusion improves the physical and biological properties of the glass. The paper also briefly presents recent progress in titanium phosphate glass processing, which allows the development of viable commercial applications in various biomedical fields.

2. Phosphate-based glass structure

Phosphate glasses are inorganic polymers based on the tetrahedral phosphate anion $[PO_4]^{3-}$, which is linked to form a three-dimensional network [36]. The phosphate tetrahedra are classified by the number of oxygen atoms shared with other phosphate tetrahedra, which are termed bridging oxygens (BOs). This classification is denoted by Q^n terminology, where Q refers to the phosphorus atom bonded to four oxygen atoms forming a tetrahedron and n refers to the number of BOs per tetrahedron and ranges from zero to three [3,36,37]. The structure of vitreous P_2O_5 consists of only Q^3 phosphate tetrahedra, which form a three-dimensional network. However, owing to the highly hygroscopic and volatile nature of P_2O_5, it becomes necessary to incorporate modifying oxides. This results in depolymerization of the glass network via the cleavage of P−O−P bonds and the formation of negatively charged non-bridging oxygens (NBOs) at the expense of BOs. The NBOs coordinate the modifier cations such that the cations attain their preferred coordination number with respect to oxygen [3,36,37].

Significant work has been carried out on a range of binary systems as a way of probing the effect of monovalent and divalent ion additions on the glass structure. Of particular note is the paper by Kirkpatrick & Brow [3], which shows the correlation between Q^n species and Na_2O content. However, while giving significant structural insight into the phosphate network, these glasses possess limited technological application.

Of more technological interest is the development of ternary systems such as the $Na_2O{-}CaO{-}P_2O_5$ system, which has been investigated extensively [12,38,39], and also the Na_2O–Fe_2O_3–P_2O_5 system [40], an extension of the developmental work on the binary Fe_2O_3–P_2O_5 system [41] as a possible system for the encapsulation of nuclear waste.

For the $Na_2O-CaO-P_2O_5$ system, compositions were investigated either side of the metaphosphate composition [12] and dissolution rates shown to be strongly influenced by the CaO content, with dissolution rates varying from 1.57×10^{-4} to 2.83×10^{-3} mg cm^{-2} h^{-1}. However, of more significance is the fact that these glasses give rise to quite significant changes in pH with time in distilled water, which has implications for cell survival. This was exemplified by the work of Bitar *et al.* [42], who showed that direct cell growth on ternary $Na_2O-CaO-P_2O_5$ glasses, some with very high CaO content, was significantly inhibited even with suitable buffers in the cell culture medium. This has driven the need to develop glasses with either significantly lower dissolution rates and/or more controlled pH changes with time.

3. Probing the structure of phosphate-based glasses

A whole range of techniques exist to probe the structure of glasses. Conventional X-ray diffraction will produce broad features from the disordered structure. It can confirm the presence of any crystalline components through the presence of any sharp diffraction peaks. High-energy diffraction can be used to probe the local structure through the Fourier transform (FT) of the diffraction pattern to give the radial distribution function, which, through its decomposition into the partial distribution functions, provides information about the local coordination of atoms. Complementing diffraction are a range of spectroscopic studies, which are mostly local probes that provide information largely about the structure on the order of nearest neighbour and next nearest neighbour. The vibrational techniques of Fourier transform infrared (FTIR) and Raman spectroscopy are widely used. X-ray spectroscopic (XAS) techniques are element specific and the spectral features reflect the nature of the local coordination. Nuclear magnetic resonance (NMR) is also an element-specific local probe that has been widely used in phosphate glasses.

4. Fourier transform infrared and Raman spectroscopies

FTIR and Raman spectroscopies are based on absorption and scattering of electromagnetic radiation at different wavenumbers owing to resonance vibrations of different chemical groups of a molecule. The two techniques are routinely used to confirm the various structural units present in glasses, which helps to explain the variation in the thermophysical properties of phosphate glasses as a function of composition.

Absorption of infrared radiation causes transitions in the resonant vibrational and rotational states associated with the ground electronic state of a molecule. These resonant modes of the bonds are either stretches (changes in bond length) or bends (changes in bond angles), which are typically observable in the infrared part of the spectrum. Peaks at various wavenumbers in an FTIR spectrum can readily be assigned to chemical groups because each bond or group of atoms has different vibrational energies [43].

The wavenumber in a Raman spectrum, however, is obtained by subtracting the wavenumber of the scattered radiation from that of the laser (called the Raman shift). As laser radiation hits a molecule, a proportion of the deflected

photons emerge with slightly different wavenumbers. This is due to the absorption or emission of the energy from or to the laser radiation by the molecule as a result of interactions with bond vibrations [44].

The Raman spectra of phosphate glasses occur generally in two main regions (600–1500 cm^{-1} and 0–600 cm^{-1}). The characteristic features of the phosphate network are limited to the high-wavenumber region of the spectrum (600–1500 cm^{-1}), which corresponds to the stretching vibrations of anions. This also can be divided into two subgroups: the band in the 1000–1400 cm^{-1} range, which is attributed to the terminal P−O stretching vibrations, and the band found in the 600–850 cm^{-1} range, which corresponds to bridging stretching modes [45,46]. The ratio of these may be used as a way of determining the phosphate chain length in certain glass compositions, but is not necessarily applicable in all compositions owing to the formation of ring structures rather than just linear chains.

A particular chemical group will give rise to peak(s) at the same wavenumber(s) in both Raman and FTIR spectra. In a molecule with a centre of symmetry, those vibrations symmetrical about the centre of symmetry are active in the Raman and inactive in the infrared; those vibrations that are asymmetric are inactive in the Raman and usually active in the infrared. Hence, peaks that absorb weakly in the mid-FTIR region will absorb strongly in the Raman region and vice versa. The two techniques therefore provide complementary information to each other [44].

Investigation of the vibrational behaviour of various binary, ternary and more complex phosphate glasses showed shifts in the υ_s(POP), $\upsilon_s(PO_2)$ and $\upsilon_{as}(PO_2)$ vibrations, indicating depolymerization of the phosphate chains as a result of increasing the metal oxide content [1,18,21,36,47–57]. These shifts in phosphate chains were also consistent with the corresponding Q species changes observed from NMR studies.

It was shown that, by addition of TiO_2, the symmetric stretching band of P–O–P shifts to higher frequencies. The higher wavenumber of the P−O−P band is due to the smaller P−O−P bond angle, which results from either shorter phosphate chain length or smaller metal cation size [53].

In titanium metaphosphate glasses, for example, it was shown that, as the Ti^{4+} content increases, the intensity of the bands associated with Q^2 groups at approximately 1270 and 900 cm^{-1} decreases relative to those associated with Q^1 groups at approximately 1100 and 1000 cm^{-1}. A small shift of the υ_{as} (P−O−P) band to a higher energy with an increase in the Ti^{4+} content was also observed [18].

5. Magic angle spinning nuclear magnetic resonance

NMR offers significant opportunities to probe phosphate-based glasses and has been widely developed and used as both a spectroscopic and an imaging technique. In particular, solid-state NMR can offer a wealth of information on glass structure. The obvious starting point for phosphate-based glasses is to use ^{31}P NMR. ^{31}P has a large magnetic moment and hence one of the highest receptivities of any nucleus [58]. These nuclear properties coupled with its 100 per cent natural abundance makes ^{31}P a very sensitive nucleus. It is a spin-1/2 nucleus and so is most strongly affected by the chemical shielding interaction,

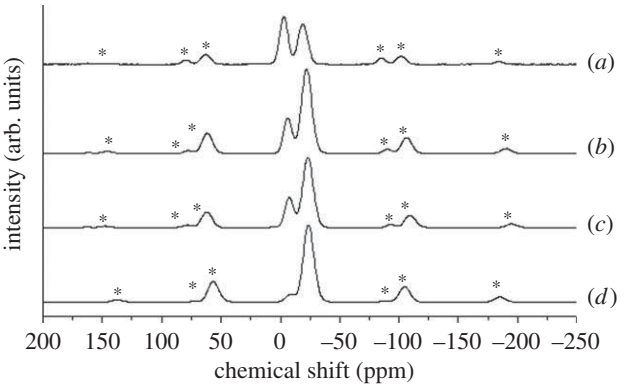

Figure 1. ^{31}P MAS NMR spectra for glass samples of compositions (*a*) 45 mol% P_2O_5 8 mol% CaO 47 mol% Na_2O, (*b*) 45 mol% P_2O_5 12 mol% CaO 43 mol% Na_2O, (*c*) 45 mol% P_2O_5 35 mol% CaO 20 mol% Na_2O and (*d*) 45 mol% P_2O_5 40 mol% CaO 14 mol% Na_2O. The change in the $Q^1 : Q^2$ ratio can clearly be seen. The asterisks denote spinning sidebands.

which is a result of the electronic density around the nucleus modifying the magnetic field experienced by the nucleus. This changes the resonance frequency of the nucleus and is termed the chemical shift, and is usually quoted in parts per million to remove the magnetic field dependence. This interaction is spatially dependent such that, in a powder sample, a broadened powder lineshape is produced that reflects the symmetry of the local environment. When there are multiple phosphorus sites, the broadening caused by the anisotropy produces severe overlap between the different environments, which often prevents unambiguous resolution of the different sites. The common approach is to use magic angle spinning (MAS) with the powder sample rotated rapidly (many kHz) at 54.7° to the main static magnetic field, which removes the anisotropy, greatly improving the resolution. In such spectra, the Q^n species can be distinguished on the basis of their differing isotropic chemical shifts. The static lineshapes break up under MAS into the isotropic line and a series of spinning sidebands that are separated from the isotropic line by multiples of the spinning rate. The intensity contribution from the spinning sidebands must be included in determining the relative abundance of each site. NMR offers resolution of the local environments in both crystals and glasses despite the broader lines glasses as a result of the greater isotropic linewidths owing to the increased chemical shift dispersion, which results from the disorder in the structure. ^{31}P MAS NMR experiments offer direct information about the Q^n speciation and have been used in binary, ternary and more complex systems [59,60]. An example is shown in figure 1 where, at the compositions shown, Q^1 and Q^2 species are dominant. However, further information may also be obtained from the isotropic chemical shifts, to give information on the changing local arrangements in the glass owing to the effects on the bonding of different metals in the system coordinating to the phosphate network. For example, as sodium and calcium change their relative bonding to the phosphate tetrahedra. The shift ranges and the effects on ^{31}P are well defined [3,19,36,47,58,61]. The distribution of Q^n species provides valuable information as to the range of environments. In phosphate glasses usually a binary model is observed, which means that at any

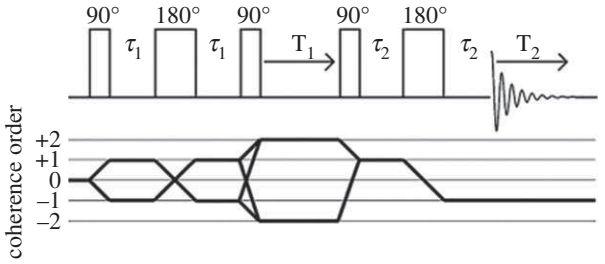

Figure 2. The refocused INADEQUATE experiment used to detect ^{31}P–^{31}P connectivity in phosphates.

given composition only two consecutive Q^n species are found, as opposed to a purely random distribution, where all Q^n species would be present simultaneously with a statistical distribution in these species. An alternative description of the network connectivity N_{P-O-P} is given by

$$N_{P-O-P} = \sum_{n=0}^{3} n f_n,$$

where f_n is the fractional intensity of that Q^n species [19].

More advanced experiments can be carried out on phosphorus, often enabled via its high sensitivity and high abundance. Phosphorus nuclei can interact with one another via their nuclear spins, either directly (the through space dipolar coupling) or indirectly via electron spins in the bonds (the through bond or J-coupling). The J-couplings, although often not resolvable, can be quantitatively determined by a spin–echo refocusing of the effect under chemical shift offsets as found in disordered samples. Connectivity information from correlation experiments has been increasingly applied to glassy phosphate materials. In the ^{31}P two-dimensional refocused INADEQUATE (figure 2) experiment, the various Q^n peaks might be connected to another and these appear as cross peaks in the two-dimensional spectrum. In the INADEQUATE spectrum, nuclei in sites that are J-coupled via a BO give rise to cross peaks equidistant from the double quantum frequency = 2 × single quantum frequency line. This allows the separate chains of PO_4 tetrahedra to be distinguished. The improved resolution arising from a dispersion of the peaks in the second dimension also allows an accurate fit of the one-dimensional MAS lineshape.

A whole series of papers demonstrate the utility of related two-dimensional experiments that can reveal, in complex ^{31}P MAS NMR spectra, which peaks belong to the same phase, the order of the connectivity and even the chain length [62–64]. This has been further developed in the REINE experiment, in which the two-dimensional distributions of both $^2JP;P$ (two bond) couplings and spin–echo dephasing times (T_{02}) were observed that could be correlated with changes in the ^{31}P chemical shift [65]. These variations in $^2JP;P$ constitute a potentially rich new source of information for the characterization of variations in bond angle and bond length. The observed spectral features, especially the distributions of parameters, can be compared with first principle calculations of J-couplings [66].

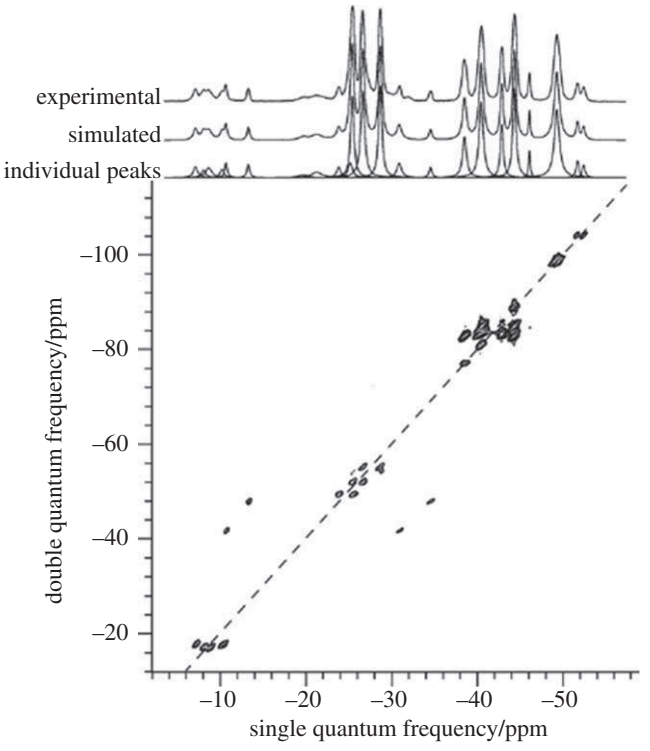

Figure 3. ^{31}P MAS NMR data along with the two-dimensional INADEQUATE data of $(P_2O_5)_{50}(CaO)_{30}(Na_2O)_{10}(TiO_2)_{10}$ [68].

In crystalline systems, the narrower resonances under MAS and the longer lifetimes of the resonances (T_2) mean that the two-dimensional sequences are generally more straightforward. Examples of such work in these systems have included unravelling quite complex phase mixtures with many phosphorus sites in two fully crystallized glasses to form sodium calcium metaphosphate ceramics [67]. Of high relevance here is the partial crystallization of some low-content titanium-, strontium- and zinc-containing glasses. The correlation experiments work on both crystalline and glassy systems so they can separate these phases and provide information on the connectivity in both. In the crystallized titanium composition examined ($(P_2O_5)_{50}(CaO)_{30}(Na_2O)_{10}(TiO_2)_{10}$), three crystalline phases were identified by a combination of X-ray diffraction and ^{31}P one-dimensional and two-dimensional INADEQUATE NMR [68]. Figure 3 shows the NMR data. The main phase present was identified as $NaCa(PO_3)_3$, while TiP_2O_7 and β-CaP_2O_7 were also found to be present in smaller amounts. A total of 23 ^{31}P peaks were observed in this sample. The three distinct phosphorus sites linked together as a repeating chain of PO_4 units in the $NaCa(PO_3)_3$ phase are clearly visible near the centre of the INADEQUATE spectrum (figure 3) as three pairs of cross peaks at the expected positions. The cubic titanium pyrophosphate phase TiP_2O_7 has eight sites in the one-dimensional MAS NMR spectrum at a relatively low chemical shift (ranging from −38 to −53 ppm). The β-$Ca_2P_2O_7$ phase appears in the INADEQUATE spectrum as two separate

pairs of cross peaks, which arise from the two P_2O_7 dimer species. Further, at relatively low intensity is a phase that has been referred to as 'P6' containing a chain of six distinct phosphorus sites [67]. In the one-dimensional spectrum, two remaining ^{31}P peaks occur at −19.8 and −21.3 ppm. These peaks are absent from the refocused INADEQUATE spectrum, indicating that they are not directly linked to any of the other phosphorus sites. A more detailed description of this sample is given in O'Dell *et al.* [68]. Interestingly, in the zinc-containing phase, there was a strong residual glassy component that could be readily seen in both the one-dimensional and two-dimensional NMR data.

Many of these phosphate systems of interest are based on sodium calcium phosphates with the titanium as a minor component. Hence it is also possible to obtain data from ^{23}Na MAS NMR. Sodium is another 100 per cent abundant NMR-active isotope, but has a spin-3/2 so experiences the nuclear quadrupolar interaction [58,69 and references therein]. The presence of the quadrupolar interaction makes spectra more complex to interpret, but can provide additional information on the coordination environments associated with neighbouring network formers and modifiers [38,70]. The quadrupolar interaction introduces a magnetic field-dependent effect through the second-order perturbation [58,69]. Hence by recording spectra at multiple applied magnetic fields and either simulating spectra using computer programs such as Quadfit [71] or plotting the change in the centre of gravity position of the lineshape the interactions can be deduced [22,72,73].

The other nuclei typically in these systems are much less accessible to solid-state NMR. The most commonly studied of these remaining nuclei is ^{17}O. Direct spectroscopic probes of the local environment around oxygen can provide extremely important information. The NMR active isotope ^{17}O is unfortunately only 0.037 per cent naturally abundant. It has $I = 5/2$ so is also a quadrupolar nucleus, but it has also been shown to have a large chemical shift range that makes it a good discriminator of different chemical sites even with residual quadrupolar broadening. To make it accessible, isotopic enrichment is usually necessary. In phosphates, the covalent nature of the bonds tends to make the quadrupolar interaction quite large and hence the lines even at high field and under fast MAS quite broad [58,74]. The number of reports of ^{17}O of phosphates is still limited, but has grown significantly in the last few years. This probably results from the relatively large coupling constants ^{17}O experiences in phosphates with χ_Q [58,69] of approximately 4 MHz in NBOs, compared with BOs, which have $\chi_Q \sim 7.5$ MHz [75,76]. Such large values only really become accessible with the availability of high fields and faster MAS rates. In phosphates, quantification of BO and NBO has been shown in a number of studies to be consistent between ^{31}P- and ^{17}O-derived NMR data. The chemical discrimination of oxygen can add a new dimension to the information provided by NMR on such glasses.

The remaining two nuclei are more demanding still. Both ^{43}Ca and $^{47,49}Ti$ are quadrupolar nuclei that fall into the category termed 'low-γ' because of their small magnetic moments [77]. This essentially means that the nuclei resonate at low Larmor frequencies that lead to poor intrinsic sensitivity and that any second-order quadrupolar effects are much more pronounced. ^{43}Ca has low natural abundance (0.135%) and a nuclear spin of 7/2. Although spectra can be obtained at natural abundance at moderate magnetic field using large-volume rotors [78],

usually high fields are needed to separate sites. This has been demonstrated in apatite, in which the two inequivalent calcium sites can be resolved [79]. More advanced sequences such as ^{1}H–^{43}Ca REDOR confirmed the assignment by looking at the differing relative proximity of the two calcium sites to the proton in the structure [79]. ^{43}Ca MAS NMR at natural abundance for a sodium calcium phosphate sol–gel prepared glass was compared with hydroxyapatite and pseudo-wollastonite [80]. ^{43}Ca NMR confirmed the difference in calcium environments, with the signal in the sol–gel at a significantly different chemical shift from the two model samples. Titanium is also a very demanding low-γ nucleus with two NMR-active isotopes, ^{47}Ti and ^{49}Ti. Both are quadrupolar with spins of 5/2 and 7/2, respectively, with the broadening of ^{47}Ti being 3.52 greater than ^{49}Ti, so that it is the latter isotope that is usually observed [58,81]. The significant complication is that the two isotopes are separated by only a few kilohertz, which means that the lineshapes of the two isotopes often overlap. The only report from titanium phosphates has been from some layered crystalline titanium phosphates [82], and, to date, there are no data from titanium-containing phosphate glasses.

6. X-ray absorption spectroscopy

X-ray absorption spectroscopy (XAS) is an element-specific technique that allows the characterization of the local environment and electronic structure of particular atoms in a wide range of materials. Synchrotron X-ray radiation can provide the energy ranges and brightness required to investigate most elements in the periodic table [83]. XAS probes the electronic transitions from core states in the absorbing atom. XAS spectra are usually considered in two parts: the X-ray absorption near-edge structure (XANES) region, which can provide information on local symmetry around the excited element and its speciation, and the extended X-ray absorption fine structure (EXAFS) region, at threshold energies greater than those required for electron release, which provides spatial information on local chemical environments (the chemical nature of neighbouring atoms, together with coordination shell distances and numbers). Analysis of the XANES region can return the coordination geometry and oxidation state of the absorbing atom. Data in the EXAFS region are usually modelled using curved-wave theory [84] in order to determine neighbouring atom types, distances and coordination numbers. Figure 4 shows a generalized view of an XAS spectrum.

As with all techniques, XAS has a number of advantages and limitations. It is particularly suited to the study of dilute elements, where the data can be collected in fluorescence mode to avoid self-absorption of the signal, and can also be used in reflection to study molecules on surfaces. Common limitations are the difficulty in determining coordination numbers with an accuracy of greater than $\pm 20\%$ and the interference between absorption edges from elements of similar Z in the same sample. Furthermore, because the coordination numbers and static/thermal disorder parameters are correlated, it is generally not possible to extract correlation numbers to better than $\pm 1/2$ atom in a glassy material. The use of XAS in the study of metal-doped glasses has been particularly fruitful when applied to elements such as Fe, Ti and Ga within what is otherwise a significantly lower atomic number matrix [85–87]. Recent developments in data

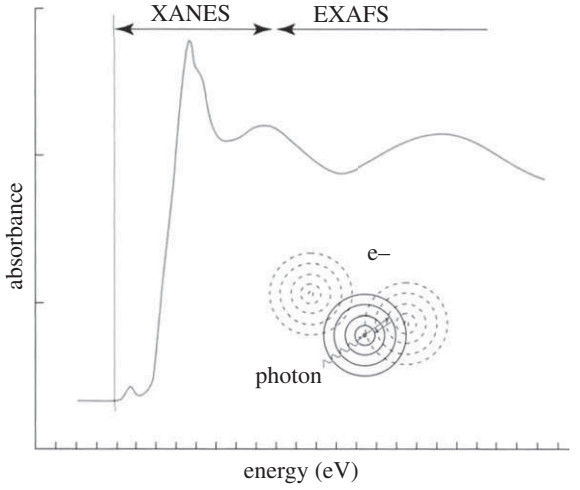

Figure 4. Generalized XAS spectra showing the relationship between XANES and EXAFS in the spectra.

collection mean that time resolution in the picosecond range is now possible at third-generation synchrotron sources [88]. This allows the measurement of a wide range of dynamics, including many of interest in the field of biomaterials.

7. Ti X-ray absorption near-edge structure

Ti K-edge XANES data usually exhibit three peaks at energies just before the main absorption edge. These pre-peaks have been assigned as follows: one to the $1s \rightarrow 3d$ transition and two to the $1s \rightarrow \mathrm{Ti}3d/O2p$ transitions, which are mainly t_{2g} in character [89,90]. The lowest energy $1s \rightarrow \mathrm{Ti}3d/O2p$ peak has been shown to be very sensitive to changes in the coordination environment of titanium, shifting to a lower energy and becoming more intense as the Ti coordination changes from six- to five- to fourfold [91]. This peak is usually the focus of structural analysis. The local coordination of titanium in the bioresorbable metaphosphate $P_2O_5{-}CaO{-}Na_2O{-}TiO_2$ glass system was investigated using Ti K-edge XANES [85]. It was shown that the titanium ions occupy an octahedral structural environment with minimal distortion in all the glass compositions. The pre-edge feature in the XANES spectra from the 3 mol% TiO_2-doped sample soaked in distilled water for various times was shown to be very similar, suggesting that the titanium environment is stable in water over long periods of time. This is in agreement with the fact that titanium is known to improve the chemical durability of phosphate glasses.

8. Neutron and X-ray scattering

Both neutron and X-ray scattering are valuable tools in the study of Ti-doped phosphate glasses. Scattering data are collected at the appropriate source: a reactor or spallation source for neutrons, and usually a synchrotron source

for X-rays, although high-energy laboratory-based sources are now available. The data are then corrected for absorption and multiple scattering and then normalized. The corrected data are Fourier transformed to obtain a real-space pair-distribution function (PDF) that contains information about every atomic correlation in the glass structure. Modelling of the PDF provides atom type, atomic distances, coordination numbers and thermal parameters for the short-range correlations. Assignment of the various features in the PDF necessary for this modelling process is made easier if both X-ray and neutron data are available from the same sample since atoms scatter X-rays and neutrons with different strengths. This complementary nature of X-ray and neutron scattering has been exploited in the study of $TiO_2-P_2O_5$ [59] and $TiO_2-CaO-Na_2O-P_2O_5$ glasses [92]. In order to obtain information on the many overlapping longer range correlations, a structural model of the glass which is consistent with the scattering data has to be built. Reverse Monte Carlo (RMC) modelling is one approach to this and has been applied to titanium-containing phosphate glasses [59].

9. Synthesis methods

Phosphate-based glasses are extremely simple to synthesize via conventional melt routes. They have relatively low fusion temperatures and readily form glasses without devitrification. The biggest technological hurdle is the inclusion of phosphorus without using excessive amounts of pure P_2O_5, which can pick up significant amounts of water on exposure to air in a very short time and is also volatile at high temperatures and can lead to losses during melting and changes in the expected composition [93]. Usually the phosphorus is added as a stable oxide containing one of the modifying cations, e.g. $CaHPO_4$ or NaH_2PO_4. Any remaining phosphorus required is then added as P_2O_5. To limit problems with water uptake (and also P_2O_5 loss owing to volatilization), melting can be easily performed in either ampoules or covered crucibles, depending on the purity required.

The sol–gel process serves as a useful alternative to the conventional melt–quench process used for producing glasses. The main advantages of this process—which involves the reaction of inorganic alkoxide and metal chloride precursors to form a colloid through hydrolysis and polycondensation reactions and subsequent thermal treatment to yield a dense, porous, glassy material—are its high level of adaptability and the low temperatures involved (up to an order of magnitude lower than in the melt–quench process). The process of reacting from a liquid allows sol–gel glasses to be deposited as thin films on a substrate, drawn into fibres or produced as micrometre- or nanometre-sized spherical particles, while the low processing temperature allows the incorporation of active biological ingredients such as proteins, antibiotics and chemotherapeutic molecules into the glass structure [94].

Silica-based sol–gel glasses have been studied extensively; however, few studies have focused on the synthesis of phosphate-based glasses by the sol–gel route and even fewer on the synthesis of sol–gel titanium phosphate glasses. This can mainly be attributed to the non-trivial chemistry involved in phosphate sol–gel synthesis. Alkyl phosphates undergo hydrolysis at considerably slower rates than alkyl silicates, and the times required for synthesis and subsequent drying are of the

order of several weeks. Nonetheless, the synthesis of sol–gel titanium phosphate glasses has progressed, with a significant improvement in the understanding of both the synthesis and their physical properties.

The phosphate precursor of choice for these sol–gels is $PO(OH)_{3-x}(OR)_x$ (R = alkyl group), which can be reacted with a titanium alkoxide to yield a sol at equimolar P/Ti ratios; ^{31}P MAS NMR results reveal the presence of P−O−Ti bonds without the occurrence of precipitation at the expense of gelation [95,96]. Neutron and X-ray diffraction data for binary P_2O_5–TiO_2 glasses prepared using *n*-butyl phosphate and titanium isopropoxide as precursors show that the glass structure comprises TiO_6 octahedra and PO_4 tetrahedra (the latter present as isolated P_2O_7 groups) that are linked by corner-sharing to form a three-dimensional amorphous network; RMC simulations provided a model of the glass structure that is similar to the superstructure of crystalline TiP_2O_7 at the nearest-neighbour level [19]. In comparison, ternary CaO–TiO_2–P_2O_5 glasses consist of chains and rings of PO_4 tetrahedra that are linked to each other by bonds between Ca^{2+} ions and NBOs and are linked to TiO_6 octahedra via corner-sharing oxygen atoms [85]. The comparison of binary P_2O_5−TiO_2 glasses of the same composition prepared by sol–gel and melt–quench routes provides several interesting results [60]. For instance, in the sol–gel glass, the Ti^{4+} ion has an average coordination number of 6 and tends to form TiO_6 octahedra, whereas, in the melt-derived glass, the same ion has an average coordination number of between 4 and 5 since it exists predominantly in the fourfold and fivefold coordination states as TiO_4 tetrahedral and TiO_5 pyramidal units, respectively, while only a small number of Ti^{4+} ions are present as TiO_6 octahedra. The higher coordination number in the sol–gel glass coincides with its higher refractive index and density when compared with the melt–quenched glass. Furthermore, the Ti–O bond length in the melt-derived glass is slightly shorter than that in the sol–gel glass; this may possibly be attributed to the presence of TiO_5 pyramidal units in the melt-derived glass in addition to the TiO_4 tetrahedral and TiO_6 octahedral units.

Thus, the results seemingly indicate that, for a binary P_2O_5−TiO_2 glass, sol–gel processing provides a more consistently ordered structure than is possible by melt–quenching, although the effect of such differences on the biocompatibility of the resulting glasses has not been studied. In addition, no reports exist in the literature regarding similar comparisons for ternary P_2O_5−CaO−TiO_2 or quaternary P_2O_5−CaO−Na_2O−TiO_2 glasses, and considering the wealth of data available for melt–quenched quaternary titanium glasses, a focus on these compositional phase diagrams via sol–gel routes and in particular the quaternary P_2O_5−CaO−Na_2O−TiO_2 glasses would be of interest.

10. Titanium pyrophosphate glasses

Navarro *et al.* [97] carried out one of the first extensive investigations, including physicochemical, morphological and structural analysis, of phosphate glasses containing up to 8 mol% TiO_2 in *in vitro* degradation studies in simulated body fluid (SBF). As TiO_2 was incorporated into the ternary phosphate glass with an equimolar content of P_2O_5 and CaO (44.5 mol%), in general an improvement in the chemical durability of the glass was observed. Weight loss studies showed that,

while the glass containing no TiO_2 underwent greater than 1.6 per cent weight loss after immersion in SBF over a 112 day period and greater than 11 per cent weight loss after immersion in distilled water over an 80 day period, the glasses containing 5 and 8 mol% TiO_2 underwent considerably lower weight losses of greater than 0.3 per cent in SBF and approximately 1 per cent in distilled water over the same periods. This was suggested to be related to the structural changes generated by the incorporation of titanium ions into the phosphate network, which can be observed in the Raman spectra as a change in the phosphate network from chain-extending Q^2 tetrahedra to chain-terminating Q^1 groups. Also, the Raman spectra confirmed the presence of TiO_5 and TiO_6 units in the glass structure with increasing TiO_2 content. Hence, the addition of TiO_2 to the ternary phosphate glass increases the O/P ratio and creates stronger Ti−O−P cross-linking within the glass network, which makes the glass denser and more resistant to degradation. Furthermore, TiO_2 incorporation affected the mechanical properties of the glasses, with the elastic modulus increasing from 66.6 GPa for the TiO_2-free glass to 75.95 GPa for the 8 mol% TiO_2 glass.

Measurement of the dissolution of the glasses in distilled water for compositions $0.45P_2O_5{-}0.24CaO{-}(0.31-x)Na_2O{-}xTiO_2$, where x ranges from 0.05 to 0.25, showed that the solubility is higher in glasses that are Ti-free or have low-titanium content. Thus, while the 0 mol% TiO_2 glass shows a weight loss of approximately 0.14 mg cm^{-2} following immersion in deionized water over a 500 hour period, the 25 mol% TiO_2 glass shows a weight loss of approximately 0.03 mg cm^{-2} over the same period. In addition, the Young modulus of the studied glasses increases slightly with the TiO_2 content from approximately 50.8 MPa at $TiO_2 = 0$ mol% to approximately 52.1 GPa at $TiO_2 = 2.5$ mol%. It was concluded that, at low concentrations (0.5 mol%), TiO_2 acts as a network modifier; however, the further addition of TiO_2 leads to a change in the network from chain-extending Q^2 tetrahedra to chain-terminating Q^1 units. The measured pH and Ca^{2+} release also confirmed the degradation results [98].

Investigation of the solubility and bioactivity of titanium pyrophosphate glasses showed that the addition of titanium into the ternary phosphate glass reduced the solubility owing to structural rearrangements as titanium is added, leading to a glass more resistant to hydration [99]. In another more detailed structural analysis of the $P_2O_5{-}CaO{-}Na_2O{-}TiO_2$ glass system in the pyrophosphate region using FTIR and FT–Raman spectroscopies, the TiO_2 enters the glass network, with TiO_4 tetrahedra connected to PO_4 tetrahedra through a P−O−Ti bond. It was also shown that CaO acts as a cross-linker by forming Ca−O−P bonds [100].

11. Titanium metaphosphate glasses

For additions of up to 5 mol% TiO_2 to metaphosphate glasses containing 30 mol% CaO, it was shown that the density increased significantly with TiO_2 content. This was attributed to the closer packing of atoms owing to the formation of strong P−O−Ti bonds. The increased density was also correlated with an increase in T_g, a measure of the glass bulk properties, which is believed to be due to the formation of TiO_4 and TiO_5 units and again P−O−Ti bonds that form ionic cross-linking between the NBOs of two different chains and strengthen the glass structure. The degradation and ion release rate were demonstrated to be significantly reduced

by addition of TiO_2 up to 5 mol%; thus, the degradation rate for a TiO_2-free glass immersed in deionized water over a 672 hour period was $400 \times 10^{-6}\%\,mm^{-2}\,h^{-1}$, whereas that for the 5 mol% TiO_2 glass under the same conditions was almost two orders of magnitude lower at $6 \times 10^{-6}\%\ mm^{-2}\,h^{-1}$ [101].

In 2009, Abou Neel *et al.* [18] investigated the doping of a high CaO content (40 mol%) metaphosphate glass with TiO_2 up to 5 mol%. The results were consistent with those from previous studies [101]. However, it was shown that the smallest addition of TiO_2 to phosphate glasses containing 40 mol% CaO produced considerably higher density and T_g along with a lower degradation rate than a similar metaphosphate glass system with 30 mol% CaO.

Incorporation of up to 15 mol% titanium into the metaphosphate glass was achieved. The degradation rate and ion release study showed an increase with time and a significant decrease owing to the addition of titanium. Interestingly, the same trend was observed for Ti^{4+}, with the lowest Ti^{4+} release found in the glass with the highest titanium content. An increase in both T_g and density was also observed with TiO_2 incorporation, which could be associated with the formation of TiO_5 and TiO_6 titanate polyhedra between the phosphate glass chains [24].

Another example of the strong effect of titanium additions is given by the study of $(P_2O_5)_{0.45}(CaO)_{0.3}(Na_2O)_{0.25-x}(TiO_2)_x$ $(0 \le x \le 0.15)$. Across this compositional range, the degradation rate decreased by a factor of 200 from $400 \times 10^{-6}\%\,mm^{-2}\,h^{-1}$ for the TiO_2-free glass to $2 \times 10^{-6}\%\,mm^{-2}\,h^{-1}$ for the 15 mol% TiO_2 glass. This can be directly related to the increase in the network connectivity of the phosphate from 1.56 to 1.95 across this series [22]. It is interesting to compare the competing effects on network connectivity of the three metals sodium, calcium and titanium, which suggests that high connectivity and hence stability can be obtained in phosphates through a combination of calcium and titanium.

After crystallization of titanium phosphate glasses, using a heat treatment cycle selected on the basis of data from differential thermal analysis (DTA), various mixtures of α- and β-$Ca_2P_2O_7$ (β-DCP), $CaTi_4(PO_4)_6$ and TiP_2O_7 phases were identified [102] and broadly correlated with the oxide content. The β-$Ca_2P_2O_7$ (β-DCP) and $CaTi_4(PO_4)_6$ phases have been reported to be biocompatible and bioactive, respectively [103–105]. TiP_2O_7 and α-$Ca_2P_2O_7$ previously were demonstrated to have positive effects on the growth of osteoblast-like cells [106].

In summary, the general changes that occur on adding TiO_2 to phosphate-based glasses are to significantly improve the durability of the glass and this occurs by Ti occupying an octahedral conformation and forming Ti−O−P cross-links. This manifests itself as significantly increased glass transition temperatures and also significantly reduced dissolution rates. However, this occurs only up to a certain percentage, presumably owing to a limit on the number of bonds that can form.

12. Titanium phosphate glasses and biocompatibility

Investigation of the biocompatibility of phosphate glasses containing TiO_2 has used one or more of the following three approaches: (a) *in vitro* evaluation following immersion in artificially prepared fluids such as citric acid, Tris buffer,

Tris-HCl or SBF; (b) *in vitro* cell culture and subsequent assays to estimate cell viability, adhesion, proliferation, differentiation and toxicity as well as gene expression; and (c) *in vivo* implantation in various animal models and subsequent histological studies.

The first approach is by far the most commonly used. In particular, SBF—a mixture of Na^+, K^+, Mg^{2+}, Ca^{2+}, Cl^-, HCO_3^-, HPO_4^{2-} and SO_4^{2-} ions in ion-exchanged and distilled water at concentrations approximately equal to those in human plasma—affords the simplest initial evaluation of bioactivity via qualitative and quantitative assessment of surface changes (most notably the formation of apatite) in contact with the fluid [99,107]. At the same time, it is worth noting that the lack of apatite formation for a particular glass composition upon SBF immersion needs not be strictly indicative of a lack of bioactivity; indeed, some materials can directly bond with bone tissue without apatite formation [108,109]. Several titanium glass compositions have been found incapable of apatite formation, yet their biocompatibility and bioactivity have been confirmed via cell culture studies and even *in vivo* implantation [56,110,111]. Thus, although SBF immersion studies may be useful as a preliminary test, further cell culture studies are generally required to gain a better understanding of material biocompatibility.

In vitro cell culture studies represent the logical next step in understanding material biocompatibility since they provide valuable qualitative and quantitative data regarding the ability of cells to adhere and proliferate on the material surface. At a basic level, the culturing of MC3T3-E1 preosteoblast cells on $P_2O_5{-}CaO{-}Na_2O{-}TiO_2$ glasses results in DNA, RNA and total protein concentrations on the glass surface that are indicative of normal proliferation and differentiation rates [112]. The role played by the glass composition in determining how cells attach and proliferate on the glass surface is more precisely studied via various cell culture assays. The morphology of the titanium glass surface may exert significant influence on cell proliferation, with rough and highly porous samples inhibiting cell proliferation over relatively short time scales [113].

In general, a higher titanium oxide content is associated with improved cell viability, attachment and proliferation [24,101,113–115]. This is confirmed by gene expression studies, which reveal significant upregulation of important bone cell markers such as COLIA1, alkaline phosphatase, osteonectin and Cbfa-1 [110]. However, this is generally true up to a certain threshold concentration; further increases in TiO_2 content beyond this threshold were shown not to contribute towards a further increase in the glass bioactivity [101]. The inter-relationships between the glass composition, structural properties, degradation behaviour and biocompatibility provide a wealth of information for biomaterials researchers, who may use subtle variations in glass chemistry to elicit highly specific cellular responses. Indeed, quaternary $P_2O_5{-}Na_2O{-}CaO{-}TiO_2$ glasses have been doped with additional metal oxides possessing proven antimicrobial properties, such as ZnO [25] and SrO [116,117], and highly favourable results have been obtained.

In comparison with the above *in vitro* approaches, the *in vivo* implantation approach has been the subject of relatively few studies, which is to be expected given the challenges associated with regulatory and ethics approval. Either rat models or rabbit models are used, with the defect site being filled with glass granules of predefined size, with implantation times in the range of 5–12 weeks

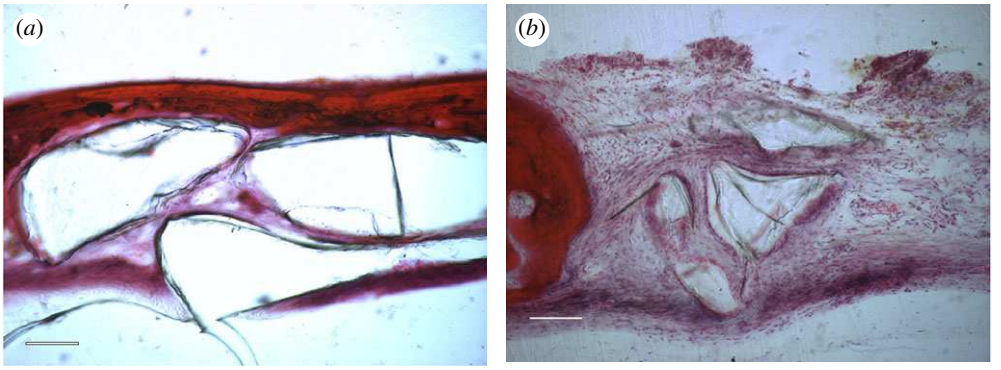

Figure 5. (*a*) Samples implanted for five weeks doped with 3% TiO_2 and (*b*) 5% TiO_2 highlighting the difference in tissue formation achieved [110]. Scale bars, (*a*,*b*) 100 µm. (Online version in colour.)

(figure 5). As in the case of *in vitro* cell culture studies, titanium glass solubility has a significant effect on *in vivo* glass behaviour with glasses that have lower dissolution rates undergoing degradation to a much lesser extent in physiological environments. It has been demonstrated that a combination of solution-mediated and cell-mediated processes serves as the driving force behind *in vivo* glass degradation [118]. The glass solubility also drives the extent to which new bone tissue may be formed around the implant, with lower dissolution rate titanium glasses being fully surrounded by new bone tissue whereas more soluble Ti-free glasses show some voids and/or soft tissue formation. Increasing the TiO_2 content—again only up to around 5 mol%—yields improvements in terms of bone cell growth [110,119].

Thus, the results of numerous studies on titanium phosphate glass biocompatibility are highly encouraging. In comparison with glasses of other compositions, those containing TiO_2 are largely found to degrade much more slowly both in simulated *in vitro* environments and in *in vivo* physiological environments; this makes the glasses more favourable from the viewpoints of cell attachment, growth, proliferation and differentiation. The next logical step would be to proceed towards human clinical trials, although there are many challenges to be overcome in designing commercially viable medical applications before such a step can be contemplated. Nonetheless, these favourable results have provided the impetus for researchers to conduct further studies focusing on the development of such medical applications.

13. Future prospects: titanium phosphate glass fibres and spheres

The potential range of biomedical applications of glass fibres encompasses the fields of muscle and ligament tissue engineering and nerve regeneration; this is mainly because the morphology and chemistry of glass fibres can be conducive to the growth of muscle tissue or neuronal cells along the longitudinal axis of the fibre. Several studies have investigated the production of phosphate glass fibres containing metallic oxides such as Fe_2O_3 and CuO

as dopants. In these studies, the glass fibres are prepared by drawing from a melt of specific viscosity at a high temperature onto a rotating steel drum. Very few studies, however, have investigated the fabrication of glass fibres made from phosphate glasses incorporating titanium oxide. One such study produced $P_2O_5-CaO-MgO-Na_2O-TiO_2$ fibres by the preforming technique at 600–620°C at a pull rate of $6\,m\,min^{-1}$ [120]. These fibres were then combined with a macromer/HEMA (methacrylic acid 2-hydroxyethylester) mixture to form degradable fibre-reinforced polymer composite matrices. The similarities between the matrices and cortical bone in terms of bending strengths and elastic moduli and the favourable biocompatibility of the matrices as evidenced by *in vitro* cell culture studies demonstrated the promise of these fibre composites for use in bone fixation devices. Proof of concept for the fabrication of $50P_2O_5-30CaO-9Na_2O-3SiO_2-3MgO-K_2O-TiO_2$ glass fibres by the preforming approach [121] has been shown. Fibres free from crystallization were successfully obtained at diameters in the range 37–173 μm, although the biocompatibility of these fibres was not reported.

Glass microspheres show considerable potential for use in a whole host of biomedical applications, including cancer radiotherapy and thermotherapy, drug and protein delivery, and bone filler materials. Microspheres can be prepared from melt–quenched glasses by a flame spheroidization process wherein glass powders are introduced into a horizontal or vertical gas/oxygen flame and then collected at specific distances from the flame. Alternatively, bioactive glass microspheres can be prepared from sol–gel glasses [94] by an emulsion technique and potentially by electrospraying as well. We envisage the application of these microspheres as an effective bone filler material; another possible application could be as a substrate in bioreactors for cell growth and differentiation.

The EPSRC are thanked for enabling the extensive UCL–Kent–Warwick collaboration on developing and understanding phosphate-based glasses. The NMR equipment used in this research received funding from EPSRC, BBSRC, the University of Warwick and Birmingham Science City Projects supported by Advantage West Midlands and the European Regional Development Fund. This work was supported in part (J.C.K.) by the WCU Programme through the National Research Foundation of Korea funded by the Ministry of Education, Science and Technology (no. R31-10069).

References

1 Shih, P. Y., Yung, S. W. & Chin, T. S. 1999 FTIR and XPS studies of P2O5–Na2O–CuO glasses. *J. Non-Cryst. Solids* **244**, 211–222. (doi:10.1016/S0022-3093(99)00011-3)

2 Shih, P. Y., Yung, S. W. & Chin, T. S. 1998 Thermal and corrosion behavior of P2O5–Na2O–CuO glasses. *J. Non-Cryst. Solids* **224**, 143–152. (doi:10.1016/S0022-3093(97)00460-2)

3 Kirkpatrick, R. J. & Brow, R. K. 1995 Nuclear-magnetic-resonance investigation of the structures of phosphate and phosphate-containing glasses: a review. *Solid State Nucl. Magn. Reson.* **5**, 9–21. (doi:10.1016/0926-2040(95)00042-O)

4 Knowles, J. C. 2003 Phosphate based glasses for biomedical applications. *J. Mater. Chem.* **13**, 2395–2401. (doi:10.1039/b307119g)

5 Abou Neel, E. A. *et al.* 2005 Effect of iron on the surface, degradation and ion release properties of phosphate-based glass fibres. *Acta Biomater.* **1**, 553–563. (doi:10.1016/j.actbio.2005.05.001)

6 Abou Neel, E. A., Ahmed, I., Pratten, J., Nazhat, S. N. & Knowles, J. C. 2005 Characterisation of antibacterial copper releasing degradable phosphate glass fibres. *Biomaterials* **26**, 2247–2254. (doi:10.1016/j.biomaterials.2004.07.024)

7 Ahmed, I., Collins, C. A., Lewis, M. P., Olsen, I. & Knowles, J. C. 2004 Processing, characterisation and biocompatibility of iron-phosphate glass fibres for tissue engineering. *Biomaterials* **25**, 3223–3232. (doi:10.1016/j.biomaterials.2003.10.013)

8 Clement, J., Manero, J. M., Planell, J. A., Avila, G. & Martinez, S. 1999 Analysis of the structural changes of a phosphate glass during its dissolution in simulated body fluid. *J. Mater. Sci. Mater. Med.* **10**, 729–732. (doi:10.1023/A:1008927222081)

9 van Wazer, J. 1950 Structure and properties of the condensed phosphates. II. A theory of the molecular structure of sodium phosphates glasses. *J. Am. Chem. Soc.* **72**, 644–647. (doi:10.1021/ja01158a002)

10 van Wazer, J. R. & Holst, K. A. 1950 Structure and properties of the condensed phosphates. I. Some general considerations about phosphoric acids. *J. Am. Chem. Soc.* **72**, 639–644. (doi:10.1021/ja01158a001)

11 Ahmed, I. *et al.* 2007 The structure and properties of silver-doped phosphate-based glasses. *J. Mater. Sci.* **42**, 9827–9835. (doi:10.1007/s10853-007-2008-9)

12 Ahmed, I., Lewis, M., Olsen, I. & Knowles, J. C. 2004 Phosphate glasses for tissue engineering. I. Processing and characterisation of a ternary-based P_2O_5–CaO–Na_2O glass system. *Biomaterials* **25**, 491–499. (doi:10.1016/S0142-9612(03)00546-5)

13 Ahmed, I., Lewis, M., Olsen, I. & Knowles, J. C. 2004 Phosphate glasses for tissue engineering. II. Processing and characterisation of a ternary-based P_2O_5–CaO–Na_2O glass fibre system. *Biomaterials* **25**, 501–507. (doi:10.1016/S0142-9612(03)00547-7)

14 Ahmed, I., Parsons, A., Jones, A., Walker, G., Scotchford, C. & Rudd, C. 2010 Cytocompatibility and effect of increasing MgO content in a range of quaternary invert phosphate-based glasses. *J. Biomater. Appl.* **24**, 555–575. (doi:10.1177/0885328209102761)

15 Ahmed, I., Ready, D., Wilson, M. & Knowles, J. C. 2006 Antimicrobial effect of silver-doped phosphate-based glasses. *J. Biomed. Mater. Res. Part A* **79**, 618–626. (doi:10.1002/jbm.a.30808)

16 Parsons, A. J., Burling, L. D., Scotchford, C. A., Walker, G. S. & Rudd, C. D. 2006 Properties of sodium-based ternary phosphate glasses produced from readily available phosphate salts. *J. Non-Cryst. Solids* **352**, 5309–5317. (doi:10.1016/j.jnoncrysol.2006.08.043)

17 Parsons, A. J., Evans, M., Rudd, C. D. & Scotchford, C. A. 2004 Synthesis and degradation of sodium iron phosphate glasses and their *in vitro* cell response. *J. Biomed. Mater. Res. Part A* **71A**, 283–291. (doi:10.1002/jbm.a.30161)

18 Abou Neel, E. A., Pickup, D. M., Valappil, S. P., Newport, R. J. & Knowles, J. C. 2009 Bioactive functional materials: a perspective on phosphate-based glasses. *J. Mater. Chem.* **19**, 690–701. (doi:10.1039/b810675d)

19 Pickup, D. M., Ahmed, I., Guerry, P., Knowles, J. C., Smith, M. E. & Newport, R. J. 2007 The structure of phosphate glass biomaterials from neutron diffraction and P-31 nuclear magnetic resonance data. *J. Phys. Condens. Matter* **19**, 415116. (doi:10.1088/0953-8984/19/41/415116)

20 Pickup, D. M., Valappil, S. P., Moss, R. M., Twyman, H. L., Guerry, P., Smith, M. E., Wilson, M., Knowles, J. C. & Newport, R. J. 2009 Preparation, structural characterisation and antibacterial properties of Ga-doped sol–gel phosphate-based glass. *J. Mater. Sci.* **44**, 1858–1867. (doi:10.1007/s10853-008-3237-2)

21 Valappil, S. P. *et al.* 2009 Controlled delivery of antimicrobial gallium ions from phosphate-based glasses. *Acta Biomater.* **5**, 1198–1210. (doi:10.1016/j.actbio.2008.09.019)

22 Kiani, A., Cahill, L. S., Abou Neel, E. A., Hanna, J. V., Smith, M. E. & Knowles, J. C. 2010 Physical properties and MAS-NMR studies of titanium phosphate-based glasses. *Mater. Chem. Phys.* **120**, 68–74. (doi:10.1016/j.matchemphys.2009.10.023)

23 Valappil, S. P. *et al.* 2008 Antimicrobial gallium-doped phosphate-based glasses. *Adv. Funct. Mater.* **18**, 732–741. (doi:10.1002/adfm.200700931)

24 Abou Neel, E. A. & Knowles, J. C. 2008 Physical and biocompatibility studies of novel titanium dioxide doped phosphate-based glasses for bone tissue engineering applications. *J. Mater. Sci. Mater. Med.* **19**, 377–386. (doi:10.1007/s10856-007-3079-5)

25 Abou Neel, E. A., O'Dell, L. A., Smith, M. E. & Knowles, J. C. 2008 Processing, characterisation, and biocompatibility of zinc modified metaphosphate based glasses for biomedical applications. *J. Mater. Sci. Mater. Med.* **19**, 1669–1679. (doi:10.1007/s10856-007-3313-1)

26 Franks, K., Abrahams, I. & Knowles, J. C. 2000 Development of soluble glasses for biomedical use. I. *In vitro* solubility measurement. *J. Mater. Sci. Mater. Med.* **11**, 609–614. (doi:10.1023/A:1008949527695)

27 Knowles, J. C., Rehman, I. & Bonfield, W. 1994 Spectroscopic and crystallographic analysis of the solution kinetics of a range of soluble phosphate based bioactive glasses. *Bioceramics.* **7**, 85–90.

28 Cartmell, S. H., Doherty, P. J., Rhodes, N. P., Hunt, J. A., Healy, D. M. & Gilchrist, T. 1998 Haemocompatiblity of controlled release glass. *J. Mater. Sci. Mater. Med.* **9**, 1–7. (doi:10.1023/A:1008830025416)

29 Cartmell, S. H., Doherty, P. J., Hunt, J. A., Healy, D. M. & Gilchrist, T. 1998 Soft tissue response to glycerol-suspended controlled-release glass particulate. *J. Mater. Sci. Mater. Med.* **9**, 773–777. (doi:10.1023/A:1008923523428)

30 Salih, V., Franks, K., James, M., Hastings, G. W., Knowles, J. C. & Olsen, I. 2000 Development of soluble glasses for biomedical use Part II. The biological response of human osteoblast cell lines to phosphate-based soluble glasses. *J. Mater. Sci. Mater. Med.* **11**, 615–620. (doi:10.1023/A:1008901612674)

31 Franks, K., Abrahams, I., Georgiou, G. & Knowles, J. C. 2001 Investigation of thermal parameters and crystallisation in a ternary $CaO–Na_2O–P_2O_5$-based glass system. *Biomaterials* **22**, 497–501. (doi:10.1016/S0142-9612(00)00207-6)

32 Knowles, J. C., Franks, K. & Abrahams, I. 2001 Investigation of the solubility and ion release in the glass system $K_2O–Na_2O–CaO-P_2O_5$. *Biomaterials* **22**, 3091–3096. (doi:10.1016/S0142-9612(01)00057-6)

33 Franks, K., Salih, V., Knowles, J. C. & Olsen, I. 2002 The effect of MgO on the solubility behavior and cell proliferation in a quaternary soluble phosphate based glass system. *J. Mater. Sci. Mater. Med.* **13**, 549–556. (doi:10.1023/A:1015122709576)

34 Mulligan, A. M., Wilson, M. & Knowles, J. C. 2003 Effect of increasing silver content in phosphate-based glasses on biofilms of *Streptococcus sanguis*. *J. Biomed. Mater. Res. Part A* **67A**, 401–412. (doi:10.1002/jbm.a.10052)

35 Mulligan, A. M., Wilson, M. & Knowles, J. C. 2003 The effect of increasing copper content in phosphate-based glasses on biofilms of *Streptococcus sanguis*. *Biomaterials* **24**, 1797–1807. (doi:10.1016/S0142-9612(02)00577-X)

36 Brow, R. K. 2000 Review: the structure of simple phosphate glasses. *J. Non-Cryst. Solids* **263**, 1–28. (doi:10.1016/S0022-3093(99)00620-1)

37 Walter, G., Vogel, J., Hoppe, U. & Hartmann, P. 2001 The structure of $CaO–Na_2O–MgO–P_2O_5$ invert glass. *J. Non-Cryst. Solids* **296**, 212–223. (doi:10.1016/S0022-3093(01)00912-7)

38 Deffontaines, B., Montagne, L., Vast, P. & Palavit, G. 1991 Characterisation of crystalline species during the preparation of phosphate ceramics in the $Na_2O–CaO–P_2O_5$ system. *C. R. Acad. Sci. Ser.* **312**, 1123–1127.

39 Uo, M., Mizuno, M., Kuboki, Y., Makishima, A. & Watari, F. 1998 Properties and cytotoxicity of water soluble $Na_2O–CaO–P_2O_5$ glasses. *Biomaterials* **19**, 2277–2284. (doi:10.1016/S0142-9612(98)00136-7)

40 Bingham, P. A., Hand, R. J., Hannant, O. M., Forder, S. D. & Kilcoyne, S. H. 2009 Effects of modifier additions on the thermal properties, chemical durability, oxidation state and structure of iron phosphate glasses. *J. Non-Cryst. Solids* **355**, 1526–1538. (doi:10.1016/j.jnoncrysol.2009.03.008)

41 Yu, X. Y., Day, D. E., Long, G. J. & Brow, R. K. 1997 Properties and structure of sodium-iron phosphate glasses. *J. Non-Cryst. Solids* **215**, 21–31. (doi:10.1016/S0022-3093(97)00022-7)

42 Bitar, M., Salih, V., Mudera, V., Knowles, J. C. & Lewis, M. P. 2004 Soluble phosphate glasses: *in vitro* studies using human cells of hard and soft tissue origin. *Biomaterials* **25**, 2283–2292. (doi:10.1016/j.biomaterials.2003.08.054)

43 Drake, A. F. 1994 Optical spectroscopy. In *Microscopy, optical spectroscopy, and macroscopic techniques* (eds C. Jones, B. Mulley & A. H. Thomas), pp. 151–171. Methods in Molecular Biology, vol. 22. Totowa, NJ: Humana Press Inc.

44 Stevens, M. P. 1999 *Polymer chemistry: an introduction*, pp. 129–163. New York, NY: Oxford University Press.

45 Reis, S. T., Faria, D. L. A., Martinelli, J. R., Pontuschka, W. M., Day, D. E. & Partiti, C. S. M. 2002 Structural features of lead iron phosphate glasses. *J. Non-Cryst. Solids* **304**, 188–194. (doi:10.1016/S0022-3093(02)01021-9)

46 Le Saout, G., Simon, P., Fayon, F., Blin, A. & Vaills, Y. 2002 Raman and infrared study of $(PbO)(x)(P_2O_5)((1-x))$ glasses. *J. Raman Spectrosc.* **33**, 740–746. (doi:10.1002/jrs.911)

47 Carta, D., Pickup, D. M., Knowles, J. C., Ahmed, I., Smith, M. E. & Newport, R. J. 2007 A structural study of sol–gel and melt-quenched phosphate-based glasses. *J. Non-Cryst. Solids* **353**, 1759–1765. (doi:10.1016/j.jnoncrysol.2007.02.008)

48 Pemberton, J. E., Latifzadeh, L., Fletcher, J. P. & Risbud, S. H. 1991 Raman-spectroscopy of calcium-phosphate glasses with varying CaO modifier concentrations. *Chem. Mater.* **3**, 195–200. (doi:10.1021/cm00013a039)

49 Meyer, K. 1997 Characterization of the structure of binary zinc ultraphosphate glasses by infrared and Raman spectroscopy. *J. Non-Cryst. Solids* **209**, 227–239. (doi:10.1016/S0022-3093(96)00563-7)

50 Meyer, K. 1998 Characterisation of the structure of binary calcium ultraphosphate glasses by infrared and Raman spectroscopy. *Phys. Chem. Glasses* **39**, 108–117.

51 Hudgens, J. J., Brow, R. K., Tallant, D. R. & Martin, S. W. 1998 Raman spectroscopy study of the structure of lithium and sodium ultraphosphate glasses. *J. Non-Cryst. Solids* **223**, 21–31. (doi:10.1016/S0022-3093(97)00347-5)

52 Peitl, O., Zanotto, E. D. & Hench, L. L. 2001 Highly bioactive P_2O_5–Na_2O–CaO–SiO_2 glass-ceramics. *J. Non-Cryst. Solids* **292**, 115–126. (doi:10.1016/S0022-3093(01)00822-5)

53 Shih, P. Y. 2003 Properties and FTIR spectra of lead phosphate glasses for nuclear waste immobilization. *Mater. Chem. Phys.* **80**, 299–304. (doi:10.1016/S0254-0584(02)00516-3)

54 Karabulut, M., Metwalli, E., Day, D. E. & Brow, R. K. 2003 Mossbauer and IR investigations of iron ultraphosphate glasses. *J. Non-Cryst. Solids* **328**, 199–206. (doi:10.1016/S0022-3093(03)00367-3)

55 Shih, P. Y. & Shiu, H. M. 2007 Properties and structural investigations of UV-transmitting vitreous strontium zinc metaphosphate. *Mater. Chem. Phys.* **106**, 222–226. (doi:10.1016/j.matchemphys.2007.05.038)

56 Lucacel, R. C., Maier, M. & Simon, V. 2010 Structural and *in vitro* characterization of TiO_2–CaO–P_2O_5 bioglasses. *J. Non-Cryst. Solids* **356**, 2869–2874. (doi:10.1016/j.jnoncrysol.2010.09.019)

57 Tiwari, B., Sudarsan, V., Dixit, A. & Kothiyal, G. P. 2011 Effect of TiO_2 addition on the optical, thermo-physical, and structural aspects of sodium alumino-phosphate glasses. *J. Am. Ceramic Soc.* **94**, 1440–1446. (doi:10.1111/j.1551-2916.2010.04292.x)

58 MacKenzie, K. J. D. & Smith, M. E. 2002 *Multinuclear solid state NMR of inorganic materials.* Oxford, UK: Pergamon.

59 Pickup, D. M., Speight, R. J., Knowles, J. C., Smith, M. E. & Newport, R. J. 2008 Sol-gel synthesis and structural characterisation of binary TiO_2–P_2O_5 glasses. *Mater. Res. Bull.* **43**, 333–342. (doi:10.1016/j.materresbull.2007.03.005)

60 Tang, A. J., Hashimoto, T., Nishida, T., Nasu, H. & Kamiya, K. 2004 Structure study of binary titanophosphate glasses prepared by sol–gel and melting methods. *J. Ceram. Soc. Jpn.* **112**, 496–501. (doi:10.2109/jcersj.112.496)

61 Carta, D., Knowles, J. C., Smith, M. E. & Newport, R. J. 2007 Synthesis and structural characterization of P_2O_5–CaO–Na_2O sol–gel materials. *J. Non-Cryst. Solids* **353**, 1141–1149. (doi:10.1016/j.jnoncrysol.2006.12.093)

62 Fayon, F. *et al.* 2005 Through-space contributions to two-dimensional double-quantum J correlation NMR spectra of magic-angle-spinning solids. *J. Chem. Phys.* **122**, 194313. (doi:10.1063/1.1898219)

63 Fayon, F., Roiland, C., Emsley, L. & Massiot, D. 2006 Triple-quantum correlation NMR experiments in solids using J-couplings. *J. Magn. Reson.* **179**, 49–57. (doi:10.1016/j.jmr.2005.11.002)

64 Feike, M., Jager, C. & Spiess, H. W. 1998 Connectivities of coordination polyhedra in phosphate glasses from P-31 double-quantum NMR spectroscopy. *J. Non-Cryst. Solids* **223**, 200–206. (doi:10.1016/S0022-3093(97)00439-0)

65 Guerry, P., Smith, M. E. & Brown, S. P. 2009 P-31 MAS refocused INADEQUATE spin-echo (REINE) NMR spectroscopy: revealing J coupling and chemical shift two-dimensional correlations in disordered solids. *J. Am. Chem. Soc.* **131**, 11 861–11 874. (doi:10.1021/ja902238s)

66 Yates, J. R. 2010 Prediction of NMR J-coupling in solids with the planewave pseudopotential approach. *Magn. Reson. Chem.* **48**, S23–S31. (doi:10.1002/mrc.2646)

67 O'Dell, L. A., Guerry, P., Wong, A., Abou Neel, E. A., Pham, T. N., Knowles, J. C. & Brown, S. P. 2008 Quantification of crystalline phases and measurement of phosphate chain lengths in a mixed phase sample by P-31 refocused INADEQUATE MAS NMR. *Chem. Phys. Lett.* **455**, 178–183. (doi:10.1016/j.cplett.2008.02.070)

68 O'Dell, L. A., Abou Neel, E. A., Knowles, J. C. & Smith, M. E. 2009 Identification of phases in partially crystallised Ti-, Sr- and Zn-containing sodium calcium phosphates by two-dimensional NMR. *Mater. Chem. Phys.* **114**, 1008–1015. (doi:10.1016/j.matchemphys.2008.11.002)

69 Smith, M. E. & van Eck, E. R. H. 1999 Recent advances in experimental solid state NMR methodology for half-integer spin quadrupolar nuclei. *Prog. Nucl. Magn. Reson. Spectrosc.* **34**, 159–201. (doi:10.1016/S0079-6565(98)00028-4)

70 Stebbins, J. F., Farnan, I. & Xue, X. Y. 1992 The structure and dynamics of alkali silicate liquids. A view from NMR-spectroscopy. *Chem. Geol.* **96**, 371–385. (doi:10.1016/0009-2541(92)90066-E)

71 Kemp, T. F. & Smith, M. E. 2009 QuadFit: a new cross-platform computer program for simulation of NMR line shapes from solids with distributions of interaction parameters. *Solid State Nucl. Magn. Reson.* **35**, 243–252. (doi:10.1016/j.ssnmr.2008.12.003)

72 Kohn, S. C., Smith, M. E., Dirken, P. J., van Eck, E. R. H., Kentgens, A. P. M. & Dupree, R. 1998 Sodium environments in dry and hydrous albite glasses: improved Na-23 solid state NMR data and their implications for water dissolution mechanisms. *Geochim. Cosmochim. Acta.* **62**, 79–87. (doi:10.1016/S0016-7037(97)00318-9)

73 Kohn, S. C., Dupree, R. & Smith, M. E. 1989 A multinuclear magnetic-resonance study of the structure of hydrous albite glasses. *Geochim. Cosmochim. Acta.* **53**, 2925–2935. (doi:10.1016/0016-7037(89)90169-5)

74 Ashbrook, S. E. & Smith, M. E. 2006 Solid state O-17 NMR: an introduction to the background principles and applications to inorganic materials. *Chem. Soc. Rev.* **35**, 718–735. (doi:10.1039/b514051j)

75 Pourpoint, F., Gervais, C., Bonhomme-Coury, L., Azais, T., Coelho, C., Mauri, F., Alonso, B., Babonneau, F. & Bonhomme, C. 2007 Calcium phosphates and hydroxyapatite: solid-state NMR experiments and first-principles calculations. *Appl. Magn. Reson.* **32**, 435–457. (doi:10.1007/s00723-007-0040-1)

76 Vasconcelos, F., Cristol, S., Paul, J. F., Tricot, G., Amoureux, J. P., Montagne, L., Mauri, F. & Delevoye, L. 2008 O-17 solid-state NMR and first-principles calculations of sodium trimetaphosphate ($Na_3P_3O_9$), tripolyphosphate ($Na_5P_3O_{10}$), and pyrophosphate ($Na_4P_2O_7$). *Inorg. Chem.* **47**, 7327–7337. (doi:10.1021/ic800637p)

77 Smith, M. E. 2001 *Recent progress in solid-state NMR of low-gamma nuclei*, pp. 121–175. Annual Reports on NMR Spectroscopy, vol. 43. London, UK: Academic Press Ltd.

78 Lin, Z. J., Smith, M. E., Sowrey, F. E. & Newport, R. J. 2004 Probing the local structural environment of calcium by natural-abundance solid-state Ca-43 NMR. *Phys. Rev. B* **69**, 224107. (doi:10.1103/PhysRevB.69.224107)

79 Laurencin, D., Wong, A., Dupree, R. & Smith, M. E. 2008 Natural abundance ^{43}Ca solid-state NMR characterisation of hydroxyapatite: identification of the two calcium sites. *Magn. Reson. Chem.* **46**, 347–350. (doi:10.1002/mrc.2117)

80 Li, A. *et al.* 2011 Insights into new calcium phosphosilicate xerogels using an advanced characterization methodology. *J. Non-Cryst. Solids* **357**, 3548–3555. (doi:10.1016/j.jnoncrysol.2011.07.003)

81 Padro, D., Jennings, V., Smith, M. E., Hoppe, R., Thomas, P. A. & Dupree, R. 2002 Variations of titanium interactions in solid state NMR-correlations to local structure. *J. Phys. Chem. B* **106**, 13 176–13 185. (doi:10.1021/jp021583x)

82 Zhu, J. F., Trefiak, N., Woo, T. K. & Huang, Y. N. 2009 A Ti-47/49 solid-state NMR study of layered titanium phosphates at ultrahigh magnetic field. *J. Phys. Chem. C* **113**, 10 029–10 037. (doi:10.1021/jp901235w)

83 Yano, J. & Yachandra, V. K. 2009 X-ray absorption spectroscopy. *Photosynth. Res.* **102**, 241–254. (doi:10.1007/s11120-009-9473-8)

84 Mustre, J., Yacoby, Y., Stern, E. A. & Rehr, J. J. 1990 Analysis of experimental extended X-ray-absorption fine-structure (EXAFS) data using calculated curved-wave, multiple-scattering EXAFS spectra. *Phys. Rev. B* **42**, 10 843–10 851. (doi:10.1103/PhysRevB.42.10843)

85 Pickup, D. M., Abou Neel, E. A., Moss, R. M., Wetherall, K. M., Guerry, P., Smith, M. E., Knowles, J. C. & Newport, R. J. 2008 TiK-edge XANES study of the local environment of titanium in bioresorbable TiO2-CaO-Na2O-P2O5 glasses. *J. Mater. Sci. Mater. Med.* **19**, 1681–1685. (doi:10.1007/s10856-007-3342-9)

86 Pickup, D. M., Moss, R. M., Qiu, D., Newport, R. J., Valappil, S. P., Knowles, J. C. & Smith, M. E. 2009 Structural characterization by x-ray methods of novel antimicrobial gallium-doped phosphate-based glasses. *J. Chem. Phys.* **130**, 064708. (doi:10.1063/1.3076057)

87 Qiu, D., Moss, R. M., Pickup, D. M., Ahmed, I., Knowles, J. C. & Newport, R. J. 2008 An X-ray absorption spectroscopy study of the local environment of iron in degradable iron-phosphate glasses. *J. Non-Cryst. Solids* **354**, 5542–5546. (doi:10.1016/j.jnoncrysol.2008.08.008)

88 Li, Z. R. *et al.* 2010 X-ray absorption fine structure techniques. *Particul. Sci. Technol.* **28**, 95–131. (doi:10.1080/02726350903328944)

89 Fronzoni, G., Francesco, R., Stener, M. & Causa, M. 2006 X-ray absorption spectroscopy of titanium oxide by time dependent density functional calculations. *J. Phys. Chem. B* **110**, 9899–9907. (doi:10.1021/jp057353a)

90 Poumellec, B., Durham, P. J. & Guo, G. Y. 1991 Electronic-strucutre and X-ray absorption-spectrum of Rutile TiO_2. *J. Phys. Condens. Matter* **3**, 8195–8204. (doi:10.1088/0953-8984/3/42/014)

91 Farges, F., Brown, G. E. & Rehr, J. J. 1997 Ti K-edge XANES studies of Ti coordination and disorder in oxide compounds: comparison between theory and experiment. *Phys. Rev. B* **56**, 1809–1819. (doi:10.1103/PhysRevB.56.1809)

92 Moss, R. M., Abou Neel, E. A., Pickup, D. M., Twyman, H. L., Martin, R. A., Henson, M. D. & Newport, R. J. 2010 The effect of zinc and titanium on the structure of calcium-sodium phosphate based glass. *J. Non-Cryst. Solids* **356**, 1319–1324. (doi:10.1016/j.jnoncrysol.2010.03.006)

93 Brow, R. K., Kirkpatrick, R. J. & Turner, G. L. 1990 The short range structure of sodium-phosphate glasses. 1. MAS NMR studies. *J. Non-Cryst. Solids* **116**, 39–45. (doi:10.1016/0022-3093(90)91043-Q)

94 Pickup, D. M., Newport, R. J. & Knowles, J. C. In press. Sol–gel phosphate-based glass for drug delivery applications. *J. Biomater. Appl.* (doi:10.1177/0885328210380761)

95 Livage, J., Barboux, P., Vandenborre, M. T., Schmutz, C. & Taulelle, F. 1992 Sol–gel synthesis of phosphates. *J. Non-Cryst. Solids.* **147**, 18–23. (doi:10.1016/S0022-3093(05)80586-1)

96 Noda, K., Sakamoto, W., Kikuta, K., Yogo, T. & Hirano, S. 1997 Effect of phosphorus sources on synthesis of $KTiOPO_4$ thin films by sol–gel method. *Chem. Mater.* **9**, 2174–2178. (doi:10.1021/cm9703076)

97 Navarro, M., Ginebra, M. P., Clement, J., Martinez, S., Avila, G. & Planell, J. A. 2003 Physicochemical degradation of titania-stabilized soluble phosphate glasses for medical applications. *J. Am. Ceram. Soc.* **86**, 1345–1352. (doi:10.1111/j.1151-2916.2003.tb03474.x)

98 Rajendran, V., Devi, A. V. G., Azooz, M. & El-Batal, F. H. 2007 Physicochemical studies of phosphate based P_2O_5-Na_2O-CaO-TiO_2 glasses for biomedical applications. *J. Non-Cryst. Solids* **353**, 77–84. (doi:10.1016/j.jnoncrysol.2006.08.047)

99 Devi, A. V. G., Rajendran, V. & Rajendran, N. 2010 Structure, solubility and bioactivity in TiO2-doped phosphate-based bioglasses and glass-ceramics. *Mater. Chem. Phys.* **124**, 312–318. (doi:10.1016/j.matchemphys.2010.06.038)

100 Li, Y., Weng, W., Santos, J. D. & Lopes, A. M. 2008 Structural studies of $Na_2OTiO_2CaOP_2O_5$ system glasses investigated by FTIR and FT-Raman. *Phys. Chem. Glasses-Eur. J. Glass Sci. Technol. Part B* **49**, 41–45.

101 Abou Neel, E. A., Chrzanowski, W. & Knowles, J. C. 2008 Effect of increasing titanium dioxide content on bulk and surface properties of phosphate-based glasses. *Acta Biomater.* **4**, 523–534. (doi:10.1016/j.actbio.2007.11.007)

102 Dias, A. G., Skakle, J. M. S., Gibson, I. R., Lopes, M. A. & Santos, J. D. 2005 *In situ* thermal and structural characterization of bioactive calcium phosphate glass ceramics containing TiO_2 and MgO oxides: high temperature XRD studies. *J. Non-Cryst. Solids* **351**, 810–817. (doi:10.1016/j.jnoncrysol.2005.01.060)

103 Ribeiro, S. J. L. *et al.* 2006 1.5 μm emission and infrared-to-visible frequency upconversion in Er(+3)/Yb(+3)-doped phosphoniobate glasses. *J. Non-Cryst. Solids* **352**, 3636–3641. (doi:10.1016/j.jnoncrysol.2006.03.095)

104 Ryu, H. S., Youn, H. J., Hong, K. S., Chang, B. S., Lee, C. K. & Chung, S. S. 2002 An improvement in sintering property of beta-tricalcium phosphate by addition of calcium pyrophosphate. *Biomaterials* **23**, 909–914. (doi:10.1016/S0142-9612(01)00201-0)

105 Kitsugi, T., Yamamuro, T., Nakamura, T. & Masanori, O. 1995 Transmission electron-microscopy observations at the interface of bone and 4 types of calcium-phosphate ceramics with different calcium phosphorus molar ratios. *Biomaterials* **16**, 1101–1107. (doi:10.1016/0142-9612(95)98907-V)

106 Dias, A. G., Lopes, M. A. & Santos, J. D. 2004 Protein adsorption effect on in vitro acellular biodegradation of $CaO–P_2O_5$ glass ceramics. *Adv. Mater. Forum II.* **455–456**, 398–401. (doi:10.4028/www.scientific.net/MSF.455-456.398)

107 Kasuga, T., Sawada, M., Nogami, M. & Abe, Y. 1999 Bioactive ceramics prepared by sintering and crystallization of calcium phosphate invert glasses. *Biomaterials* **20**, 1415–1420. (doi:10.1016/S0142-9612(99)00047-2)

108 Kokubo, T. & Takadama, H. 2006 How useful is SBF in predicting in vivo bone bioactivity? *Biomaterials* **27**, 2907–2915. (doi:10.1016/j.biomaterials.2006.01.017)

109 Lee, K. Y., Park, M., Kim, H. M., Lim, Y. J., Chun, H. J., Kim, H. & Moon, S.-H. 2006 Ceramic bioactivity: progresses, challenges and perspectives. *Biomed. Mater.* **1**, R31–R37. (doi:10.1088/1748-6041/1/2/R01)

110 Abou Neel, E. A., Mizoguchi, T., Ito, M., Bitar, M., Salih, V. & Knowles, J. C. 2007 *In vitro* bioactivity and gene expression by cells cultured on titanium dioxide doped phosphate-based glasses. *Biomaterials* **28**, 2967–2977. (doi:10.1016/j.biomaterials.2007.03.018)

111 ElBatal, H. A., Khalil, E. M. A. & Hamdy, Y. M. 2009 *In vitro* behavior of bioactive phosphate glass-ceramics from the system $P_2O_5–Na_2O–CaO$ containing titania. *Ceramics Int.* **35**, 1195–1204. (doi:10.1016/j.ceramint.2008.06.004)

112 Del Valle, L. J., Navarro, M., Sepulcre, F., Ginebra, M. P. & Planell, J. A. 2003 Growth and differentiation of osteogenic cells on calcium phosphate glasses. *Eur. Biophys. J.* **32**, 269.

113 Brauer, D. S., Russel, C., Li, W. & Habelitz, S. 2006 Effect of degradation rates of resorbable phosphate invert glasses on *in vitro* osteoblast proliferation. *J. Biomed. Mater. Res. Part A* **77A**, 213–219. (doi:10.1002/jbm.a.30610)

114 Navarro, M., Ginebra, M. P. & Planell, J. A. 2003 Cellular response to calcium phosphate glasses with controlled solubility. *J. Biomed. Mater. Res. Part A* **67A**, 1009–1015. (doi:10.1002/jbm.a.20014)

115 Dias, A. G., Lopes, M. A., Cabral, A. T. T., Santos, J. D. & Fernandes, M. H. 2005 *In vitro* studies of calcium phosphate glass ceramics with different solubility with the use of human bone marrow cells. *J. Biomed. Mater. Res. Part A* **74A**, 347–355. (doi:10.1002/jbm.a.30357)

116 Lakhkar, N. J., Abou Neel, E. A., Salih, V. & Knowles, J. C. 2009 Strontium oxide doped quaternary glasses: effect on structure, degradation and cytocompatibility. *J. Mater. Sci. Mater. Med.* **20**, 1339–1346. (doi:10.1007/s10856-008-3688-7)

117 Lakhkar, N., Abou Neel, E. A., Salih, V. & Knowles, J. C. 2010 Titanium and strontium-doped phosphate glasses as vehicles for strontium ion delivery to cells. *J. Biomater. App.* **25**, 877–893. (doi:10.1177/0885328210362125)

118 Dias, A. G. *et al.* 2006 *In vivo* performance of biodegradable calcium phosphate glass ceramics using the rabbit model: histological and SEM observation. *J. Biomater. Appl.* **20**, 253–266. (doi:10.1177/0885328206052466)

119 Monem, A. S., ElBatal, H. A., Khalil, E. M. A., Azooz, M. A. & Hamdy, Y. M. 2008 *In vivo* behavior of bioactive phosphate glass-ceramics from the system P_2O_5–Na_2O–CaO containing TiO_2. *J. Mater. Sci. Mater. Med.* **19**, 1097–1108. (doi:10.1007/s10856-007-3044-3)

120 Brauer, D. S., Russel, C., Vogt, S., Weisser, J. & Schnabelrauch, M. 2008 Degradable phosphate glass fiber reinforced polymer matrices: mechanical properties and cell response. *J. Mater. Sci. Mater. Med.* **19**, 121–127. (doi:10.1007/s10856-007-3147-x)

121 Vitale-Brovarone, C., Novajra, G., Milanese, D., Lousteau, J. & Knowles, J. C. 2011 Novel phosphate glasses with different amounts of TiO_2 for biomedical applications dissolution tests and proof of concept of fibre drawing. *Mater. Sci. Eng. C Mater. Biol. Appl.* **31**, 434–442. (doi:10.1016/j.msec.2010.11.001)